Laura Orsatti[1]
Eleonora Forte[2]
Licia Tomei[1]
Marianna Caterino[3]
Antonello Pessi[1]
Fabio Talamo[1]

[1]IRBM P. Angeletti, Pomezia, Italy
[2]Department of Molecular Genetics and Microbiology, Duke University School of Medicine, Durham, NC, USA
[3]CEINGE, Biotecnologie Avanzate, Napoli, Italy

Received November 27, 2008
Revised January 16, 2009
Accepted February 12, 2009

Research Article

2-D Difference in gel electrophoresis combined with Pro-Q Diamond staining: A successful approach for the identification of kinase/phosphatase targets

The protein tyrosine phosphatase PRL-3 is an appealing therapeutic cancer target for its well described involvement in the metastasis progression. Nevertheless, very little is known about PRL-3 role in tumorigenesis. In the attempt to identify the protein target of this phosphatase we have devised a model system based on the use of highly invasive HCT116 colon cancer cells over-expressing PRL-3. We used 2-D difference gel electrophoresis combined with the fluorescence staining Pro-Q Diamond selective for phosphorylated proteins to monitor changes in the phosphorylation status of possible substrates. Proteins whose phosphorylation level was negatively affected by PRL-3 overexpression were identified by MS. Two proteins were found to be significantly dephosphorylated in this condition, the cytoskeletal protein ezrin and elongation factor 2. Ezrin has already been described as having a proactive role in cancer metastasis through control of its phosphorylation status, and the PRL-3-induced modulation of ezrin phosphorylation in HCT116 and human umblical vascular endothelial cells is the subject of a separate paper by Forte *et al.* [*Biochim. Biophys. Acta* 2008, 1783, 334–344]. The combination of 2-D difference in gel electrophoresis and Pro-Q Diamond was hence confirmed successful in analyzing changes of protein phosphorylation which enable the identification of kinase/phosphatase targets.

Keywords:
2-D Difference in gel electrophoresis / Elongation factor 2 / Ezrin / Phosphorylation / PRL-3
DOI 10.1002/elps.200800780

1 Introduction

PRL-3 protein, a small cysteine phosphatase involved in metastasis progression [1, 2], is considered as an interesting molecular marker for metastatic tumor cells [3, 4]. It has been found to be over-expressed in colon cancer metastasized to the liver [5] as well as in many other cancer types such as gastric, pancreatic, ovarian and prostate tumors, Hodgkin's lymphoma [1, 6, 7], melanomas, liver carcinoma [6, 8] and invasive breast tumor vasculature [9]. PRL-3 knockdown by RNAi abolishes the ability of metastatic colorectal carcinoma cell line to form metastasis in mice [10] while in gastric cancer cells it halts their invasion and migration independent of cellular proliferation. Finally, *in vivo* knockdown of PRL-3 suppresses the development of peritoneal metastasis in nude mice [11, 12].

PRL-3 belongs to the family of small, highly homologous protein named PRL phosphatases (PRL-1, 2 and 3) with a characteristic protein tyrosine phosphatase motif containing the catalytic triad and a carboxyl-terminal prenylation motif. PRL-3 farnesylation at this sequence leads to its localization to the plasma membrane and to the early endosomes, while nuclear localization may occur in the unmodified protein [13]. Fiordalisi *et al.* [14] demonstrated PRL-3 involvement in the stimulation of Rho signaling pathway to promote cell invasion. They observed increased levels of RhoA and RhoC in SW480 colorectal carcinoma cells expressing exogenous PRL-1 and PRL-3 and an inhibitory effect on cell motility by inhibition of the Rho kinase. They also showed activation of the serum response element transcription factor in a Rho-dependent manner, suggesting that PRL-3 regulates invasion and metastasis by directly affecting the cytoskeleton and also through the transcriptional regulation of target genes. Evidences in this direction are provided by a recent paper by Basak *et al.* [15] were they demonstrated that PRL-3 is an important cell-cycle regulator and is a direct p53 target gene.

Correspondence: Dr. Laura Orsatti, IRBM, Via Pontina km 30.600, 00040 Pomezia, Italy
E-mail: laura_orsatti@merck.com
Fax: +39-06-91093225

Abbreviations: DIGE, difference in gel electrophoresis**; EF2,** elongation factor 2**; ERM,** Ezrin/Radixin/Moesin**; FTI,** farnesyltransferase inhibitor**; PS,** pool standard

To better understand PRL-3 functions and its involvement in the tumor to metastasis progression, we have transiently transfected PRL-3 in HCT116 colon cancer cells with the aim of inducing detectable dephosphorylation of its substrates. 2-D difference gel electrophoresis (DIGE) [16, 17], which detects changes in the protein levels while retaining information on their post-translational modifications, was then used in combination with specific staining for phosphoproteins (Pro-Q Diamond) to analyze the proteome of this transient clone and potential PRL-3 substrates were searched among those proteins with altered phosphorylation patterns. Two proteins were found to be mainly dephosphorylated upon PRL-3 over-expression, namely the cytoskeletal protein ezrin and the elongation factor 2 (EF2).

2 Materials and methods

2.1 Cells

HCT116 were cultured at 37°C/5%CO_2 in McCoy's medium (Invitrogen, Carlsbad, CA, USA), supplemented with 10% FCS, antibiotics (streptomycin and penicillin 100 U/mL) and L-glutamine (2 mM).

2.2 Plasmids

The wild-type PRL-3 coding sequence (NM 032611) was amplified by PCR from a skeletal muscle cDNA library (Clontech, Mountain View, CA, USA) and inserted into BamHI and EcoRI sites of the pcDNA3 vector (Invitrogen) giving rise to the construct pCD-PRL-3wt. The correct coding region of the plasmid was confirmed by sequencing.

2.3 Transient transfection of plasmid DNA for ectopic PRL-3 over-expression

HCT116 cells were transfected with pCD-PRL-3wt or empty vector using Lipofectamine 2000 (Invitrogen) as recommended by the manufacturer in quadruplicate 10 cm plates. Following transfection (24 h), cells were treated with 0.1 mM sodium Orthovanadate (Sigma Aldrich, Chicago, IL, USA) and H_2O_2 for 30 min at 37°C/5% CO_2. The cells were washed once with PBS, detached with TEN (40 mM Tris, pH 7.5, 150 mM NaCl, 1 mM EDTA) and collected by 5 min centrifugation at $300 \times g$. The cell pellets were further washed three times with PBS, immediately frozen in liquid nitrogen and stored at −80°C.

2.4 Protein extraction and quantification

The cell pellets were resuspended in 0.5 mL of lysis buffer (30 mM Tris, pH 8.5, 7 M urea, 2 M thiourea, 4% CHAPS), subjected to sonication at 4°C for 30 s and finally clarified by centrifugation for 10 min at 4°C and $16\,000 \times g$. The supernatants were recovered and subjected to protein desalting/concentration using the 2-D Clean-Up Kit™ (GE Healthcare, Uppsala, Sweden). The pellets were resuspended in 100 μL of lysis buffer and the pH adjusted to 8.5 by addition of 0.1 N NaOH. Protein concentrations were determined using the 2-D Quant Kit™ (GE Healthcare).

2.5 CyDye labeling and semi-preparative gels

Four 10 cm-plates of pCD-wtPRL-3wt transfected cells (treated) and four 10 cm-plates of pCDNA3 empty vector transfected cells (control) were labeled with CyDye DIGE fluor minimal dyes following the standard DIGE protocol [18, 19] for a four-gel experiment. Samples were randomly labeled: two controls and two "treated" were labeled with Cy3 and two controls and two "treated" were labeled with Cy5. A pool standard (PS) was prepared by mixing equal amounts of each sample and labeled with Cy2. The protein to cyanine dye ratio was 50 μg/400 pmol with a reaction time of 30 min on ice, in the dark and finally quenched with the addition of 1 μL of 10 mM lysine for each 400 pmol of CyDye used. An aliquot of 50 μg of Cy2 labeled PS was mixed with 50 μg of a Cy3 and 50 μg of a Cy5 labeled sample, and an equal volume of 2 × sample buffer (7 M urea, 2 M thiourea, 4% CHAPS, 20 mg/mL DTT, 50 μL pharmalyte 3–10) was added at 4°C for 10 min before loading on the first dimension gel.

Two semi-preparative gels with 400 μg each of control and "treated" samples were prepared and stained with the fluorescent phosphoprotein gel stain Pro-Q Diamond (Molecular Probes, Eugene, OR, USA) which allows direct, in-gel detection of phosphate groups attached to serine, tyrosine and threonine residues. Afterwards, the semi-preparative gels were stained with Sypro Ruby for total-protein detection (Invitrogen) and finally used for spot picking.

2.6 Electrophoresis

The four mixed-samples containing the Cy2, Cy3 and Cy5 labeled proteins were cup loaded in 3–10 NL 18 cm IPG strips (GE Healthcare). IEF of the four mixed-samples was done simultaneously on an IPGphor 2 (GE Healthcare) for a total of 40 000 V h, at 20°C (300 V for 3 h, ramp to 1000 V in 6 h, ramp to 8000 V in 3 h and 8000 V for up to 4 h). The current limit was 50 μA/strip. The two samples for the semi-preparative gels were focused in a separate run but in the same IEF conditions as the DIGE samples. For cysteine reduction and alkylation the six focused strips were equilibrated in equilibration buffer (100 mM Tris, pH 8.0, 30% v/v glycerol, 2% w/v SDS, 6 M urea) containing 0.5% w/v DTT for 15 min and for further 15 min with equilibra-

tion buffer containing 4.5% w/v iodoacetamide. IPG strips were placed on the top of 12.5% SDS gels cast between low-fluorescence glass plates, and the second dimension electrophoresis was performed in a Peltier-cooled Ettan Dalt 12™ electrophoresis unit (GE Healthcare) at 2 W/gel, for 16 h at 25°C.

The Cy2, Cy3 and Cy5 images were obtained by scanning with a Typhoon 9410™ (GE Healthcare) each of the four DIGE gels at excitation/emission wavelength of 480/530 nm for Cy2, 520/590 nm for Cy3 and 620/680 nm for Cy5. These gels were removed from the plates and fixed in 50% MeOH, 10% acetic acid. After 1 h the fixing solution was replaced with fresh solution and incubation continued overnight. The semi-preparative gels were then washed three times for 15 min with water and placed for 2 h in the dark in Pro-Q Diamond staining solution. After staining the gels were washed in 50 mM sodium acetate pH 4.0, 20% ACN, and the gel image was acquired with the Typhoon 9410™ scanner (GE Healthcare) at 520/590 nm wavelengths. The gels were placed for 10 min in water and for 12 h in Sypro Ruby solution for total-protein staining, and washed with 10% MeOH, 7% acetic acid three times for 30 min each. The gels were scanned again with 480/633 nm wavelengths.

2.7 DIGE analysis

DeCyder software 5.01 (GE Healthcare) was used to compare the abundance changes between the control and treated samples. The batch processor module was used for normalization of the signals from each CyDye channel and spot detection on the 12 images from the four DIGE gels and the calculation of the volume ratio for each spot pair (Cy3:Cy2 and Cy5:Cy2 ratios). The biological variation analysis module was used to match all the 12 spot maps from the four DIGE gels and calculate the average abundance changes and paired Student's *t*-test *p*-values for the variance of these ratios for each protein pair across all four samples.

2.8 In gel digestion

Protein of interests were excised from the semi-preparative gels and placed in a 96-well plate using ProExcision spot picker from Perkin Elmer Instruments (Shelton, CT, USA). Excised spots were digested with Multiprobe liquid handler (Perkin Elmer Instruments). Gel plugs were first washed with 100 mM ammonium bicarbonate for 5 min, 100 mM ammonium bicarbonate/ACN 50/50 for 5 min and pure ACN for another 5 min. Fifty microlitres of 12 ng/μL trypsin (Promega, Madison, WI, USA) were added to each gel piece and after 45 min at 4°C the trypsin solution was replaced with 50 mM ammonium bicarbonate for 12 h at 37°C. Tryptic peptides were then extracted from the gel with 5% formic acid and dried by vacuum centrifugation. Peptides were resuspended in 0.5% acetic acid and analyzed by LC-IT-MS/MS.

2.9 MS and database search

An LCQ DECA XP-Plus IT mass spectrometer (Thermo Finnigan, San José, CA, USA) equipped with an in-house built micro-electrospray ion source coupled with a Surveyor HPLC (Thermo Finnigan) was used. Samples were loaded in an in-house packed pre-column (C18 resin, 5 μm particle size) placed before a C18 column packed in the sprayer. Peptides were separated and eluted from the column with a 0.5% acetic acid/ACN gradient (from 0.5% acetic acid/ACN 98/2 to 0.5% acetic acid/ACN 50/50 in 30 min, flow rate 1 μL/min). MS and MSMS spectra acquired in a data-dependent manner and the peak lists were generated using Bioworks 3.1 software (Thermo Finnigan). The resulting .dta files from each analysis were searched against the uniprot_sprot non-redundant database version 50.5 using Phenyx (GeneBio, Geneva, Switzerland) operating on a local server. IT was selected for instrument type, and LCQ was selected for the algorithm. Two search rounds were used both with trypsin selected as the enzyme and oxidized methionine and carbamidomethylated cysteine selected as variable and fixed modifications. In the first round one missed cleavage was allowed, and the normal cleavage mode was used. This round was selected in ''turbo'' search mode. In the second round three missed cleavages were allowed, and cleavage mode was set to half-cleaved. The minimum peptide length allowed was six amino acids, and the parent ion tolerance was 2.0 Da in both search rounds. The acceptance criteria were slightly lowered in the second round search (round 1: AC score 7.0; peptide Z-score, 7.0; peptide *p* value, 1E-7; round 2: AC score, 7.0; peptide Z-score, 6.0; peptide *p* value, 1E-6). Only proteins identified with one or more peptides with p value $<$ 1E-6 were considered to be true matches.

2.10 Antibodies

Antibodies–Anti–PhosphoTyrosine (clone 4G10) was from Upstate (Lake Placid, NY, catalog # 05–321). Anti-PhosphoERM (Ezrin/Radixin/Moesin) (Thr567) from Cell Signaling (Beverly, MA, USA, catalog # 3141) was reported to detect endogenous levels of Thr567 phosphorylated Ezrin, Thr 564 phosphorylated Moesin, Thr558 phosphorylated Radixin and to not cross-react with other related phosphoproteins such as Merlin or band 4.1. PhosphoEzrin (Tyr353) was from Cell Signaling (catalog # 3144) and reported as unable to detect phosphorylated Moesin or Radixin. The above-mentioned antibodies were hence used according to the specificity stated by the manufacturers. Peroxidase-conjugated secondary antibodies were purchased from Sigma Aldrich.

2.11 Western blot analysis

Equal amounts of proteins were resolved by 2-D and transferred to nitrocellulose membrane (Schleicher&Schuell, Dassel, Germany). Transfer was performed in Tris-glycine/methanol buffer (20% methanol in 25 mM Tris, 250 mM glycine, pH 8.3) for 1 h at 27 V constant voltage in ice using a transfer apparatus from Idea Scientific (Minneapolis, MN, USA). The filters were then blocked and probed with the appropriate primary antibody using the condition and antibody dilution as recommended by the manufacturers. Proteins were detected by horseradish peroxidase-conjugated secondary antibody (Sigma Aldrich) and ECL detection system (GE Healthcare).

3 Results

In order to identify PRL-3 targets, we transiently over-expressed the wild-type PRL-3 in HCT116 colon cancer cells and analyzed the differences between the phospho-protein patterns of the total protein extracts from PRL-3 and the mock transfected cells. We decided to use HCT116 cells mainly for their acceptable basal PRL-3 expression level, their migration/invasion potential and the availability of validated transfection protocols. PRL-3 over-expression is expected to decrease the phosphorylation level of its target(s) and, as a consequence, should shift their isoelectric point towards more basic values. This change can be detected in a 2-D gel, since the first dimension is based on IEF.

Twenty-four hours post transfection, the cells were treated with orthovanadate and then lysed in the presence of the same phosphatase inhibitor to block any phosphatase activity during lysis. 2-D difference in gel electrophoresis (2-D DIGE) was then used to compare the total cell lysate of the cells over-expressing PRL-3 (treated) with a control, obtained from cells transfected with an empty vector in four replicates. Control and treated samples along with a PS obtained by mixing equal amounts of each sample were labeled with the Cy2, Cy3 and Cy5 dyes. Randomization of Cy3 and Cy5 labeling should avoid false positives due to preferential labeling of the cyanine dyes towards some proteins. After labeling, the Cy2-labeled PS, a Cy3 and a Cy5-labeled sample were mixed and run in a single gel, for a total of four DIGE gels. One semi-preparative gel was also prepared for the control and one for the treated sample for selective phosphorylated protein staining (Pro-Q Diamond) and total protein staining (Sypro Ruby) for spot picking.

More than 3700 spots were detected in the 2-D map and 19 were significantly up- or down-regulated ($p = 0.01$, variation extent generally ranging between 2.60 and 1.10 fold change). These spots were picked and eleven individual proteins were identified by MS. By matching the Sypro Ruby against the Pro-Q Diamond images, we found that only two proteins were phosphorylated and their variation and identification are summarized in Table 1. In Fig. 1, a Cy3 image of the control sample is reported. Highlighted in the box are two series of phosphorylated spots showing the major changes upon PRL-3 over-expression. A more detailed view of these spots is reported in Fig. 2 together with the fold change measured for each of them. The spots reported in Fig. 2A were identified as ezrin, which, in our conditions, was resolved in three unphosphorylated isoforms whose abundance increased upon PRL-3 over-expression (spots 1, 2 and 3), and six phosphorylated isoforms, which, on the contrary, showed decreased abundance in cells over-expressing PRL-3 (spot 4, 5, 6, 7, 8 and 9). Among the latter, the most acidic spots (7, 8 and 9) were highly phosphorylated as shown by comparison of their Sypro Ruby and Pro-Q Diamond intensities (Fig. 2, panel A). Variation in the relative abundance of the different ezrin isoforms is clearly visible also from the 3-D-views reported in the upper panel of Fig. 2A.

The other phosphorylated protein whose intensity decreased following PRL-3 over-expression (Fig. 1, rectangle b, and Fig. 2B) was identified as EF2. It also appears as a series of spots, all corresponding to different EF2 isoforms, two of which are unphosphorylated (Fig. 2B, spots 10 and 11) and three are phosphorylated (Fig. 2B, spots 12, 13 and 14). The most acidic spot, (spot 14 in Table 1 and Fig. 2B) was the only one significantly changed in the 2-D DIGE experiment (fold change −1.78).

The additional spots whose level appeared altered in the 2-D DIGE experiments corresponded to unphosphorylated proteins. However, changes in the level of these proteins were low (data not shown), not exceeding 30%, and possibly due to the indirect effects of PRL-3 over-expression.

To confirm and further analyze the effect that PRL-3 over-expression had on ezrin, we performed 2-D Western blot analysis with the commercially available antibody anti-pTyr, anti-Ezrin-pTyr353 and anti-ERM-pThr567 (Fig. 3). While all the six phosphorylated isoforms of ezrin visibly contained pTyr residues, pTyr353 was essentially present in spots 4, 5, 6 and 7 and pThr567 mainly in spot 5. As evident from Fig. 3, PRL-3 over-expression affected the distribution of both Tyr and Thr phosphorylation. In particular, a significant decrease of the highly phosphorylated Tyr-containing isoforms (Fig. 3, panel B) was clearly observed, as well as a clear change in the distribution pattern of pThr567-containing ones highlighted by the shift of spot 5 into spots 4 and 2 in the wtPRL-3 over-expressing sample.

4 Discussion

In this study we used the 2-D DIGE technology combined with phosphoprotein selective staining and MS to analyze changes in the protein phosphorylation in cells over-expressing ectopic PRL-3 with the aim of identifying its possible targets. By this approach, we have demonstrated that ezrin and EF2 did in fact show an altered phosphorylation pattern upon PRL-3 over-expression, thus providing the first evidence that their phosphorylation status is affected by the PRL-3 phosphatase activity. The PRL-3-induced modula-

Table 1. Proteins significantly changed upon PRL-3 over-expression in HCT116 cells

Spot no.	Protein name	AC no.[a)]	Pro-Q Diamond	Average ratio [b)]	*t*-test [c)]	No. of peptides identified	% sequence coverage
1	Ezrin	P15311		1.90	5.0E−4	2	3.0
2	Ezrin	P15311		2.15	2.1E−4	12	22.4
3	Ezrin	P15311		1.57	1.3E−3	8	13.5
4	Ezrin	P15311	*Phosphorylated*	−1.42	1.3E−3	9	16.9
5	Ezrin	P15311	*Phosphorylated*	−1.28	8.2E−3	4	9.2
6	Ezrin	P15311	*Phosphorylated*	−2.59	6.0E−3	8	13.5
7	Ezrin	P15311	*Phosphorylated*	−1.93	1.1E−3	3	4.3
8	Ezrin	P15311	*Phosphorylated*	−2.14	1.3E−4	3	4.3
9	Ezrin	P15311	*Phosphorylated*	−1.86	3.0E−4	1	1.7
14	EF-2	P13639	*Phosphorylated*	−1.78	2.1E−3	6	7.2

a) Swiss-Prot database was searched.
b) Average volume ratios PRL-3 transfected/control from the different gels of the DIGE experiment.
c) Student's *t*-test *p*-values calculated using DeCyder software version 5.1.

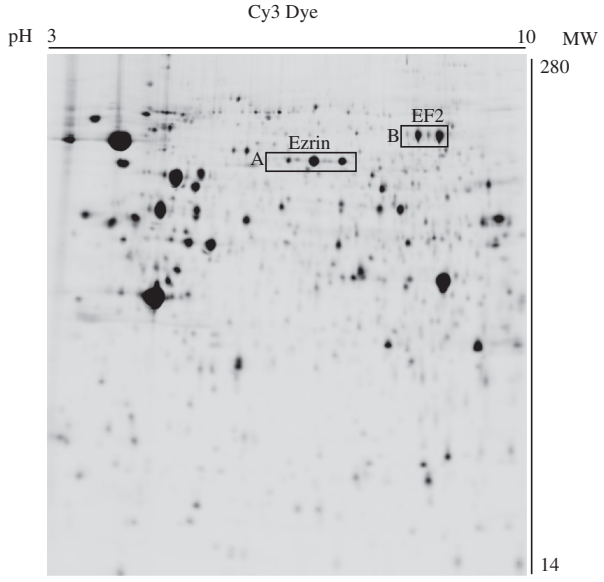

Figure 1. Cy3 dye image of 2-D gel of HCT116 total cell lysate. Highlighted in rectangle A and B are two series of spots that are changed in the 2-D DIGE experiment corresponding to ezrin and EF2, respectively.

tion of ezrin phosphorylation in HCT116 and human umblical vascular endothelial cells is the subject of a separate paper [20]. The two proteins will be discussed separately in the following paragraphs.

4.1 Ezrin

The 2-D DIGE experiments showed that the major effects induced by PRL-3 over-expression were on ezrin, particularly on its phosphorylation status. Ezrin, together with Radixin and Moesin, belongs to the ERM protein family whose function is to provide a link between the cytoplasmatic face of the plasma membrane and the actin-based cytoskeleton. It is involved in the regulation of membrane protrusions, cell-substrate adhesion and cell motility, thus playing an important role in the control of cell morphology [21–26]. Additionally, ERM proteins provide an intracellular scaffold for the formation of specialized membrane domains responsible for the transmission of signals from the extracellular space through growth factor receptors and adhesive molecules to actively regulate cell-signaling events [27, 28]. Inter- and intra-molecular associations are the major factors responsible for ezrin functions and the fine regulation of these associations is controlled by the dynamic phosphorylation of several threonine, tyrosine and serine residues. Phosphorylation of Thr567 is necessary for the protein to assume an open conformation and correctly localize to the plasma membrane [29, 30] where the activated protein can associate directly or indirectly with transmembrane proteins, adhesion molecules and ion exchangers to exploit its signaling function. Several kinases responsible for Thr567 phosphorylation have been identified so far, which basically depend on the specific membrane domain where the modification occurs [31–36].

In addition to phosphorylation at Thr567 for conformational activation and control of cell morphology, ezrin is largely phosphorylated on tyrosine and serine residues and these modifications mainly control signaling to downstream events [37–40]. Tyrosine phosphorylation has been associated to signaling pathways that can profoundly affect survival, adhesion, migration/invasion behavior, all of which are important during tumor development and progression [21, 23, 41–44].

The association of ezrin with many prometastatic pathways could partially explain the recent reports where high levels of ezrin expression were found in several systems such as metastatic rhabdomyosarcoma [45], metastatic spread of osteosarcoma, mammary and pancreatic adenocarcinomas [46–48] and androgen-regulated spreading of prostate cancer cell [49].

Our data show that ezrin is a target of PRL-3 activity, a phosphatase highly expressed in cancer metastasis. This might be of particular significance because ezrin involvement in the metastatic process has been well described and it is now clear how this role does depend on the phos-

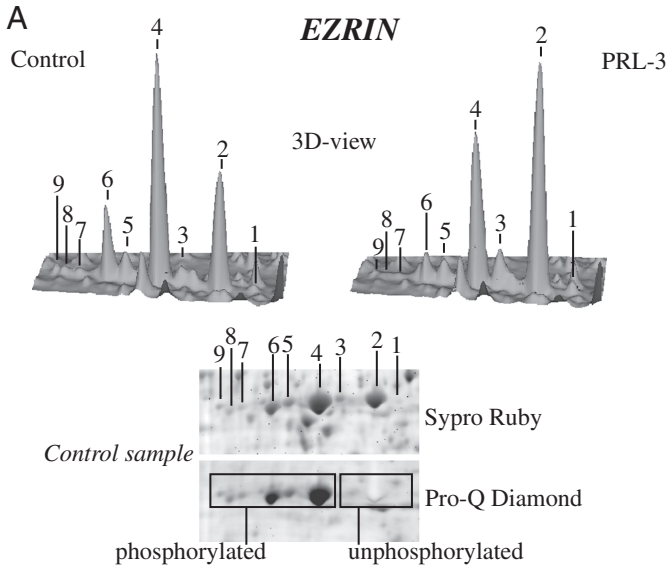

Spot	*Fold change*
1	+1.90
2	+2.15
3	+1.57
4	-1.42
5	-1.28
6	-2.59
7	-1.93
8	-2.14
9	-1.86

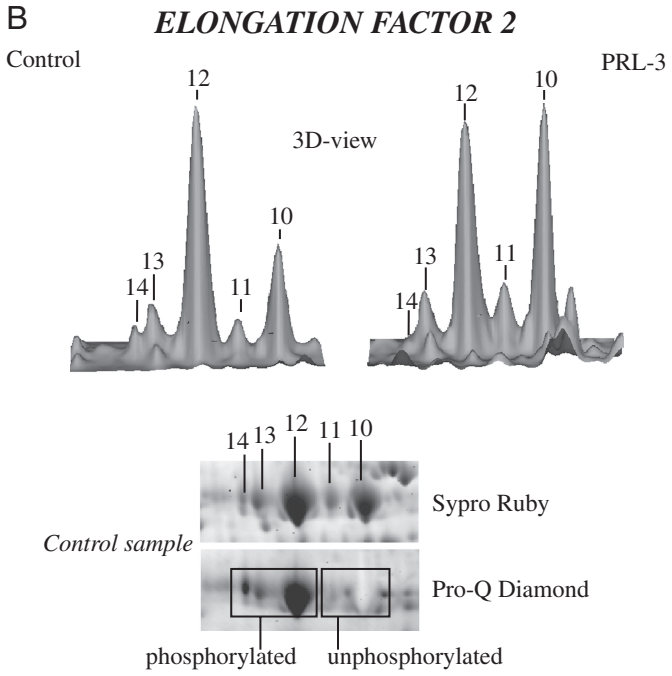

Spot	*Fold change*
10	not changed
11	not changed
12	not changed
13	not changed
14	-1.78

Figure 2. Detailed view and fold change of (A) ezrin and (B) EF2 spots. Panels A and B show the Sypro Ruby and Pro-Q Diamond staining of a control sample. Spots 1, 2 and 3 of ezrin are unphosphorylated and increase upon PRL-3 over-expression while spots 4, 5, 6, 7, 8 and 9 are phosphorylated and decrease upon PRL-3 over-expression. Spot 14 of EF2 decreases while spots 10, 11, 12 and 13 do not change significantly. 3-D-views were obtained from Cy dyes images.

phorylation/dephosphorylation status. While many kinases controlling ezrin phosphorylation have already been identified, only two phosphatases, the myosin phosphatase and PP2C, were found to regulate ERM proteins dephosphorylation [50, 51].

By 2-D DIGE experiments combined with Pro-Q Diamond and MS, ezrin was identified in HCT116 cells as a series of at least nine spots, the first three resulted to be unphosphorylated while the others showed increasing levels of phosphorylation. This complex pattern was consistent with the notion that ezrin is largely phosphorylated at threonine, tyrosine and serine residues. Upon PRL-3 over-expression all ezrin isoforms were affected, leading to a decrease of phosphorylated forms and an increase of unphosphorylated ones. A more detailed analysis of the ezrin residues whose phosphorylation status is affected by PRL-3 action and the biological indications confirming ezrin as a specific and direct target of PRL-3 have been reported elsewhere [20]. Interestingly, both ezrin and PRL-3 were found to be over-expressed in metastatic tumors, supporting our finding that PRL-3 is a regulator of ezrin phosphorylation status and that they might cooperate to induce metastatic progression.

4.2 EF2

In addition to ezrin, PRL-3 ectopic over-expression in HCT116 colon cancer cells seems to affect also the

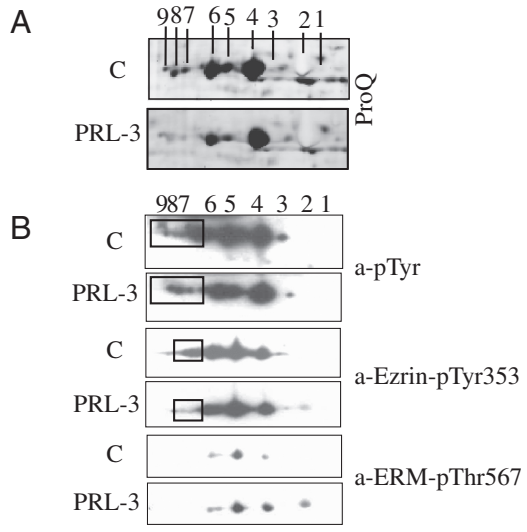

Figure 3. Western blot of ezrin spots with anti-pTyr, anti-Ezrin-pTyr353 and anti-ERM-pThr567 showing the change of the distribution pattern of pTyr, pTyr353 and pThr567 upon PRL-3 over-expression. Highlighted in the rectangles are the spots that were more affected by PRL-3 over-expression. The Pro-Q Diamond image of the corresponding spots is reported above for reference.

phosphorylation status of EF2. Eukaryotic EF2 mediates the translocation step of peptide-chain elongation in protein synthesis and its activity is regulated by phosphorylation [52]. EF2 must be dephosphorylated to be active while its phosphorylation at Thr56 stops the translation process. In fact, this modification prevents EF2 from binding to the ribosome, and, therefore, may represent the mechanism of global protein synthesis regulation at the elongation step [53].

In our phospho-2-D map, EF2 was identified as a series of five isoforms, three of which resulted to be phosphorylated while two were not. One of the two unphosphorylated forms presents a further modification, different from phosphorylation, which has not been identified so far. In HCT116 cells over-expressing PRL-3, we observed a decreased phosphorylation of the most acidic among the phosphorylated EF2 isoforms: this reduction was not reflected in a corresponding increase of one of the more basic spots. This could be explained either by degradation of EF2 after dephosphorylation or by a plausible limit of sensitivity of our system. As a matter of fact, the abundance of the unphosphorylated spots, which are those expected to increase after dephosphorylation, is higher than that of the spot observed to decrease upon PRL-3 over-expression. Therefore, in terms of spot volume, the variation level could have been very low in comparison to the total spot volume, and could have been masked by the automatic background subtraction by the DeCyder software before the statistical analysis on spot variation.

In a recent paper, it was shown that the treatment of head and neck squamous cell carcinoma cells with a farnesyltransferase inhibitor (FTI) SCH66336, designed to target tumors with mutations of the ras oncogene, whose activity mainly depends on prenylation, induced phosphorylation of EF2 [54]. Surprisingly, this effect was independent of ras-MEK-EF2 kinase and ras-PI3K/p70S6K-EF2K signaling cascades, the only mechanisms known to control the activation of EF2 kinase and therefore EF2 phosphorylation/activation. Since FTIs have shown anti-tumor activity also independently of ras [55], the authors postulated that SCH66336 might inhibit the activity of other farnesylated proteins, in this case that of a phosphatase, with the consequent reduction of EF2 dephosphorylation.

As we already mentioned, PRL-3 localization is controlled by prenylation. In particular, the prenylated form localizes at early endosomes and plasma membrane, while the unmodified one shift into the nucleus [13]. It is possible that the increased EF2 phosphorylation observed upon treatment with an FTI agent could be due to the inhibition of PRL-3 prenylation and its consequent shifts into the nucleus and subtraction from its cytosolic substrates like EF2. Further investigation would be needed to confirm this hypothesis.

In conclusion we show that through the gel-based proteomic approach reported in this paper it is possible to analyze changes of protein phosphorylation, which enable the identification of kinase/phosphatase targets.

We would like to thank Dr. Bruno Bacher from GE Healthcare for the support and helpful discussions on 2-D DIGE experiments and Janet Clench for editing the manuscript.

The authors have declared no conflict of interest.

5 References

[1] Stephens, B. J., Han, H., Gokhale, V., Von Hoff, D., *Mol. Cancer Ther.* 2005, *4*, 1653–1661.

[2] Bessette, D. C., Qiu, D., Pallen, C. J., *Cancer Metastasis Rev.* 2008, *27*, 231–252.

[3] Miskad, U. A., Semba, S., Kato, H., Yokozaki, H., *Phatobiology* 2004, *71*, 176–184.

[4] Peng, L., Ning, J., Meng, L., Shou, C., *J. Cancer Res. Clin. Oncol.* 2004, *130*, 521–526.

[5] Saha, S., Bardelli, A., Buckhaults, P., Velculescu, V. E., Rago, C., St. Croix, B., Romans, K. E., *Science* 2001, *294*, 1343–1346.

[6] Wang, Z., He, Y. L., Cai, S. R., Zhan, W. H., Li, Z. R., Zhu, B. H., Chen, C. Q. *et al.*, *Int. J. Cancer* 2008, *123*, 1439–1447.

[7] Schwering, I., Braeuninger, A., Distler, V., Jesdinsky, J., Diehl, V., Hansmann, M.-L., Rajewsky, K. *et al.*, *Mol. Med.* 2003, *9*, 85–95.

[8] Wu, X., Zeng, H., Zhang, X., Zhao, Y., Sha, H., Ge, X., Zhang, M. *et al.*, *Am. J. Pathol.* 2004, *164*, 2039–2054.

[9] Parker, B. S., Argani, P., Cook, B. P., Liangfeng, H., Chartrand, S. D., Zhang, M., Saha, S. *et al.*, *Cancer Res.* 2004, *64*, 7857–7866.

[10] Kato, H., Semba, S., Miskad, U. A., Seo, Y., Kasuga, M., Yokozaki, H., *Clin. Cancer Res.* 2004, *10*, 7318–7328.

[11] Zhao, W. B., Li, Y., Liu, X., Zhang, L.Y. *et al.*, *Int. J. Mol. Med.* 2008, *22*, 187–192.

[12] Li, Z., Zhan, W., Wang, Z., Zhu, B., He, Y., Peng, J., Cai, S. *et al.*, *Biochem. Biophys. Res. Commun.* 2006, *348*, 229–237.

[13] Zeng, Q., Si, X., Horstmann, H., Xu, Y., Hong, W., Pallen, C. J., *J. Biol. Chem.* 2000, *275*, 21444–21452.

[14] Fiordalisi, J. J., Keller, P. J., Cox, A. D., *Cancer Res.* 2006, *66*, 3153–31615.

[15] Basak, S., Jacobs, S. B., Krieg, A. J., Pathak, N., Zeng, Q., Kaldis, P., Giaccia, A. *et al.*, *Mol. Cell* 2008, *30*, 303–314.

[16] Van den Bergh, G., Arckens, L., *Curr. Opin. Biotechnol.* 2004, *15*, 38–43.

[17] Baker, M. A., Witherdin, R., Hetherington, L., Cunningham-Smith, K., Aitken, R. J., *Proteomics* 2005, *5*, 1003–1012.

[18] Alban, A., David, S. O., Bjorkesten, L., Andersson, C., Sloge, E., Lewis, S., Currie, I., *Proteomics* 2003, *3*, 36–44.

[19] Ünlü, M., Morgan, M. E., Minden, J. S., *Electrophoresis* 1997, *18*, 2071–2077.

[20] Forte, E., Orsatti, L., Talamo, F., Barbato, G., De Francesco, R., Tomei L., *Biochim. Biophys. Acta* 2008, *1783*, 334–344.

[21] Bretscher, A., Edwards, K., Fehon, R. G., *Nat. Rev. Mol. Cell Biol.* 2002, *3*, 586–599.

[22] Takeuchi, K., Sato, N., Kasahara, H., Funayama, N., Nagafuchi, A., Yonemura, S., Tsukita, S., *J. Cell Biol.* 1994, *125*, 1371–1384.

[23] Crepaldi, T., Gautreau, A., Comoglio, P. M., Louvard, D., Arpin, M., *J. Cell Biol.* 1997, *138*, 423–434.

[24] Saotome, I., Curto, M., McClatchey, A. I., *Dev. Cell* 2004, *6*, 855–864.

[25] Mackay, D. J., Esch, F., Furthmayr, H., Hall, A., *J. Cell Biol.* 1997, *138*, 927–938.

[26] Lamb, R. F., Ozanne, B. W., Roy, C., McGarry, L., Stipp, C., Mangeat, P., Jay, D. G., *Curr. Biol.* 1997, *7*, 682–688.

[27] Gautreau, A., Louvard, D., Arpin, M., *Curr. Opin. Cell Biol.* 2002, *14*, 104–109.

[28] Hiscox, S., Jiang, W. G., *J. Cell Sci.* 1999, *112*, 3081–3090.

[29] Fievet, B. T., Gautreau, A., Roy, C., Del Maestro, L., Mangeat, P., Louvard, D., Arpin, M., *J. Cell Biol.* 2004, *164*, 653–659.

[30] Matsui, Y., Maeda, M., Doi, Y., Yonemura, S., Amano, M., Kaibuchi, K., Tsukita, S., *J. Cell Biol.* 1998, *140*, 647–657.

[31] Nakamura, N., Oshiro, N., Fukata, Y., Amano, M., Fukata, M., Kuroda, S., Matsuura, Y. *et al.*, *Genes Cells* 2000, *5*, 571–581.

[32] Ng, T., Parsons, M., Hughes, W. E., Monypenny, J., Zicha, D., Gautreau, A., Arpin, M. *et al.*, *EMBO J.* 2001, *20*, 2723–2741.

[33] Tran Quang, C., Gautreau, A., Arpin, M., Treisman, R., *EMBO J.* 2000, *19*, 4565–4576.

[34] Matsui, T., Yonemura, S., Tsukita, S., *Curr. Biol.* 1999, *9*, 1259–1262.

[35] Cant, S. H., Pitcher, A., *Mol. Biol. Cell* 2005, *16*, 3088–3099.

[36] Baumgartner, M., Sillman, A. L., Blackwood, E. M., Srivastava, J., Madson, N., Schilling, J., Wright, J. H. *et al.*, *Proc. Natl. Acad. Sci. USA* 2006, *103*, 13391–13396.

[37] Zhou, R., Cao, X., Watson, C., Miao, Y., Guo, Z., Forte, J. G., Yao, X., *J. Biol. Chem.* 2003, *278*, 35651–35659.

[38] Jin, C., Ge, L., Ding, X., Chen, Y., Zhu, H., Ward, T., Wu, F. *et al.*, *Biochem. Biophys. Res. Commun.* 2006, *341*, 784–791.

[39] Heiska, L., Carpen, O., *J. Biol. Chem.* 2005, *280*, 10244–10252.

[40] Yang, H.-S., Hinds, P. W., *Cancer Res.* 2006, *66*, 2708–2715.

[41] Krieg, J., Hunter, T., *J. Biol. Chem.* 1992, *267*, 19258–19265.

[42] Srivastava, J., Elliott, B. E., Louvard, D., Arpin, M., *Mol. Biol. Cell* 2005, *16*, 1481–1490.

[43] Elliot, B. E., Qiao, H., Louvard, D., Arpin, M., *J. Cell. Biochem.* 2004, *92*, 16–28.

[44] Gautreau, A., Poullet, P., Louvard, D., Arpin, M., *Proc. Natl. Acad. Sci. USA* 1999, *96*, 7300–7305.

[45] Yu, Y., Khan, J., Khanna, C., Helman, L., Meltzer, P. S., Merlino, G., *Nat. Med.* 2004, *10*, 175–181.

[46] Khanna, C., Wan, X., Bose, S., Cassaday, R., Olomu, O., Mendoza, A., Yeung, C. *et al.*, *Nat. Med.* 2004, *10*, 182–186.

[47] Nestl, A., Von Stein, O. D., Zatloukal, K., Thies, W.-G., Herrlich, P., Hofmann, M., Sleeman, J. P., *Cancer Res.* 2001, *61*, 1569–1577.

[48] Akisawa, N., Nishimori, I., Iwamura, T., Onishi, S., Hollingsworth, M. A., *Biochem. Biophys. Res. Commun.* 1999, *258*, 395–400.

[49] Chuan, Y.-C., Pang, S.-T., Cedazo-Minguez, A., Norstedt, G., Pousette, Å., Flores-Morales, A., *J. Biol. Chem.* 2006, *281*, 29938–29948.

[50] Hishiya, A., Ohnishi, M., Tamura, S., Nakamura, F., *J. Biol. Chem.* 1999, *274*, 26705–26712.

[51] Fukata, Y., Kimura, K., Oshiro, N., Saya, H., Matsuura, Y., Kaibuchi, K., *J. Cell Biol.* 1998, *141*, 409–418.

[52] Wang, L., Proud, C. G., *FEBS Lett.* 2002, *531*, 285–289.

[53] Ryazanov, A. G., *FEBS Lett.* 2002, *514*, 26–29.

[54] Ren, H., Tai, S.-K., Khuri, F., Chu, Z., Mao, L., *Cancer Res.* 2005, *65*, 5841–5847.

[55] Feldkamp, M. M., Lau, N., Roncari, L., Guha, A., *Cancer Res.* 2001, *61*, 4425–4431.

